Please cite this article as:
Romuald Szopa, Edyta Pawlak, Jarosław Siedlecki, Stefan and Kolmogoroff models of solidification. Comparison of numerical solutions, Scientific Research of the Institute of Mathematics and Computer Science, 2008, Volume 7, Issue 1, pages 185-192.
The website: http://www.amcm.pcz.pl/

STEFAN AND KOLMOGOROFF MODELS OF SOLIDIFICATION. COMPARISON OF NUMERICAL SOLUTIONS

Romuald Szopa, Edyta Pawlak, Jarosław Siedlecki

Institute of Mathematics, Czestochowa University of Technology, Poland

Abstract. Problems connected with the mathematical description of pure metals solidification (macro approach) are often called the Stefan ones. The second generation models (micro/macro approach) discussed in this paper base on a theory presented by Kolmogoroff (Mehl-Johnson-Avrami-Kolmogoroff models). Both macro and micro/macro problems can be analyzed using the numerical methods. The aim of investigations presented here was a comparison of numerical solutions obtained by use of macro and micro/macro approach. On a stage of numerical modelling the finite difference method has been applied.

1. Governing equations

Solidification of pure metals or eutectic alloys proceeds at a constant temperature (solidification point T^*). The mathematical macroscopic model of the process discussed is called in literature 'the Stefan problem' [1-3]. The domain Ω being a sum of molten metal $\Omega_1(t)$ and solid state $\Omega_2(t)$ sub-domains is considered. The position of interface $\Gamma_{12}(t)$ is time-dependent. So the Stefan problem belongs to a group of moving boundary ones. The temperature field in domain of molten metal is described by the well known Fourier equation

$$c_1(T)\frac{\partial T_1(x,t)}{\partial t} = \nabla\left[\lambda_1(T)\nabla T_1(x,t)\right] \tag{1}$$

where c_1, λ_1 are the volumetric specific heat and thermal conductivity of material, T, x, t denote the temperature, spatial co-ordinates and time.
The similar equation determines the temperature field in a solidified part of metal

$$c_2(T)\frac{\partial T_2(x,t)}{\partial t} = \nabla\left[\lambda_2(T)\nabla T_2(x,t)\right] \tag{2}$$

where c_2, λ_2 are the volumetric specific heat and thermal conductivity of solid body.
It should be pointed out that only heat conduction in Ω is considered (it results from the form of equations (1) and (2)). On the interface $\Gamma_{12}(t)$ the following

boundary condition is taken into account

$$-\lambda_1 \frac{\partial T_1(x,t)}{\partial n} = -\lambda_2 \frac{\partial T_2(x,t)}{\partial n} + L\, v_n \tag{3}$$

where L is a volumetric latent heat, v_n is a solidification rate in a normal direction, $\partial/\partial n$ denotes a normal derivative (Figure 1). Additionally the temperatures $T_1(x,t) = T_2(x,t) = T^*$.

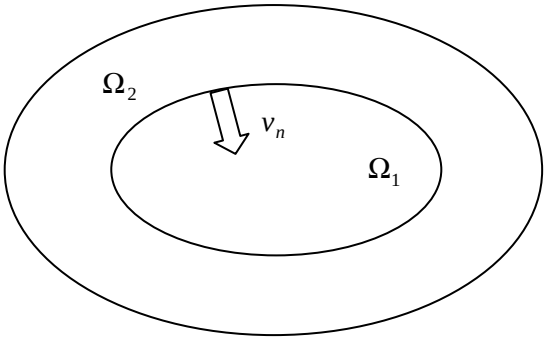

Fig. 1. Domain considered

On the outer surface of the system the boundary condition in general form

$$\Phi\left[T_2(x,t),\ \frac{\partial T_2(x,t)}{\partial n}\right] = 0 \tag{4}$$

is given. The initial temperature distribution and the initial position of interface are also known.

In literature one can find the analytical solution of this problem. They concern the very simple geometrical and boundary conditions. In a practice the problem of pure metals solidification can be solved using the numerical methods.

The other approach to the Stefan problem results from the considerations concerning the crystallization processes proceeding in a micro scale (micro/macro model of solidification). Then one considers the following energy equation

$$c(T)\frac{\partial T(x,t)}{\partial t} = \nabla\left[\lambda(T)\nabla T(x,t)\right] + L\frac{\partial f_S(x,t)}{\partial t} \tag{5}$$

where f_S is a volumetric solid state fraction at the point x.

The energy equation (5) is the typical Fourier equation with additional term (source function) controlling the evolution of latent heat L, but the capacity of internal heat sources results from the laws determining the nucleation and nuclei

growth (micro-scale). Here, the model basing on the assumption that the kinetic of nucleation and nuclei growth are proportional to the undercooling below the solidification point are discussed [3-5].

So, the function

$$\omega(x,t) = N(x,t)V(x,t) \tag{6}$$

where N - grains density [nuclei/m^3], V - a single grain volume is introduced. Denoting $u = \partial R/\partial t$ (u is a crystallization rate, R is a grain radius) we have

$$\omega(x,t) = \frac{4}{3}\pi\nu\, N(x,t)\left[\int_0^t u(x,\tau)\,\mathrm{d}\tau\right]^3 \tag{7}$$

at the same time for spherical grains $\nu = 1$, for other types of crystallization $\nu < 1$.
The exponential model of crystallization proposed by Mehl-Johnson-Avrami--Kolmogoroff bases on the formula [3-5]

$$f_S(x,t) = 1 - \exp\left[-\omega(x,t)\right] = 1 - \exp\left\{-\frac{4}{3}\pi\nu\, N(x,t)\left[\int_0^t u(x,\tau)\,\mathrm{d}\tau\right]^3\right\} \tag{8}$$

The nucleation and nuclei growth are determined by the following dependencies

$$N(x,t) = \eta\ \Delta T^2(x,t) = \eta\left[T^* - T(x,t)\right]^2 \tag{9}$$

where η is a nucleation coefficient

$$\frac{\mathrm{d}R(x,t)}{\mathrm{d}t} = \mu\ \Delta T^m(x,t) \tag{10}$$

where μ is the growth coefficient $m \in [1,2]$.
The nucleation process stops when $\Delta T(x,t+\Delta t) < \Delta T(x,t)$ [6].
In numerical realization the solution of micro/macro solidification model can be obtained in different ways (see: [6, 7]).

2. Numerical aspects of Stefan and micro/macro models solution

The Stefan problem (macro model of solidification) is solved here using the numerical procedure called a Temperature Recovery Method (TRM). The TRM is not new [3, 8] and it has been known for more then 40 years. In its initial version it was

used for numerical computations of typical Stefan problems, at present one can find the generalizations concerning more complex problems (e.g. solidification of alloys).

Let us assume (it is not necessary) that the thermophysical parameters of liquid and solidified part of domain Ω are constant and equal. The 'reserve' of temperature θ is defined as the quotient of the volumetric latent heat L to the volumetric specific heat c (more precisely to c_1), this means

$$\theta = \frac{L}{c} \tag{11}$$

The domain considered is divided into control volumes which central nodes we denote as x_i. At the moment $t = 0$ the temperature at this point corresponds to the pouring temperature as well as the temperature reserve results from (11).

On the basis of the optional numerical method we find a discrete temperature field at the set of points x_i for successive levels of time. If during the interval $\Delta t = t^{f+1} - t^f$ the temperature T_i^{f+1} at point x_i decreases below the solidification point then it is assumed that the temperature at this point is equal to T^* and the reserve of temperature must be decreased, namely $\theta_i^{f+1} = \theta_i - \Delta\theta_i^{f+1}$, where $\Delta\theta_i^{f+1} = T^* - T_i^{f+1}$. So, the temperature field obtained at time t^{f+1} is corrected in following way:

i. For the nodes in which $T_0^{f+1} > T_{cr}$, the temperature reserve θ_i is untouched and equal to its initial value. The calculated temperature T_i^{f+1} is, of course, accepted.

ii. For the nodes in which $T_i^f > T^*$ and $T_i^{f+1} < T^*$ it is assumed that $T_i^{f+1} = T^*$ and the TRM procedure is initiated.

iii. For the nodes in which $T_i^f = T^*$, $T_i^{f+1} < T^*$ and $\theta_i^{f+1} > 0$ it is assumed that $T_0^{f+1} = T^*$ and the temperature reserve is decreased according the formula: $\theta_i^{f+1} = \theta_i^f - \left(T^* - T_i^{f+1}\right)$.

iv. For the nodes in which $T_i^f \le T^*$ and $\theta_i^{f+1} \le 0$ the obtained value of temperature is accepted.

Corrected in this way temperature field in Ω illustrates the thermal state in casting domain at the moment t^{f+1}, as well as this constitutes a pseudo-initial condition for the next step of computations. The interpretation of TRM in the system enthalpy-temperature is shown in Figure 2 [9].

The main problem of micro/macro model numerical solution is connected with the source function computations. The domain considered should be divided into n control volumes ΔV_i (they, as a rule, correspond to internal cells resulting from the domain disretization). The time mesh, namely

$$0 = t^0 < t^1 < t^2 < \ldots < t^f < t^{f+1} < \ldots < t^F \ , \quad \Delta t = t^{f+1} - t^f \tag{12}$$

is also introduced.

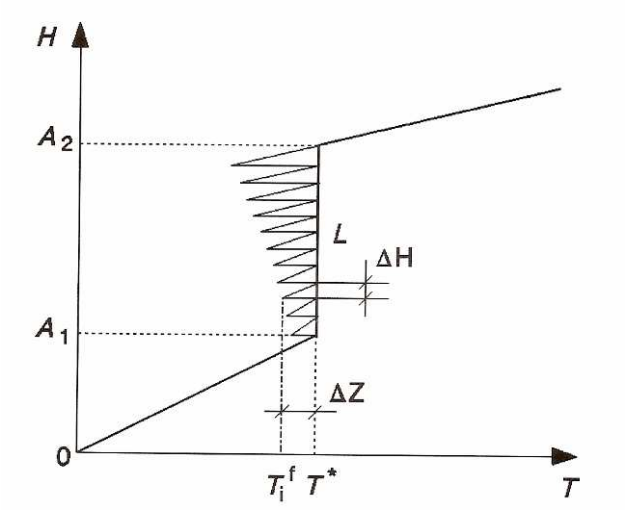

Fig. 2. Interpretation of TRM

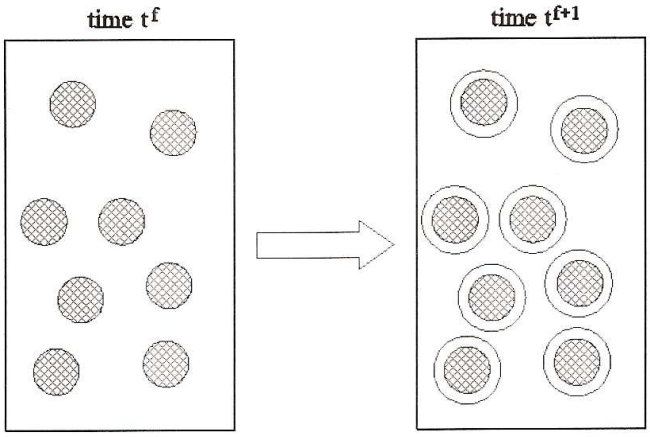

Fig. 3. Constant number of nuclei

The local temporary values of $\omega\left(\Delta V_i, t^f\right)$ result from (7). In this place the following assumptions can be introduced [4, 6]:

- a constant number of nuclei $N\left(\Delta V_i, t^f\right) = \text{const.}$ (Fig. 3),
- formula (9) is applied, but for every time step the nuclei radius is averaging,
- formula (9) is applied and the 'vicissitudes' of successive grain families are registered.

In this paper we use the simplest version of crystallization model, this means the constant number of nuclei has been taken into account.

3. Example of computations

As an example the cylindrical aluminium casting has been considered (Fig. 4).

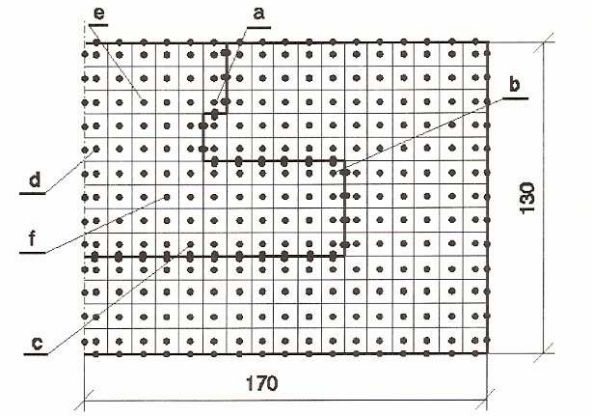

Fig. 4. Shape of domain and its discretization

The casting is produced in the typical sand mix mould. On the lateral surface of mould the Robin condition has been assumed (α = 10 W/m^{2}K), the similar condition is given on the upper surface of domain (α = 50 W/m^{2}K). The bottom plate is insulated (q = 0). The computer program for axially symmetrical domain bases on the FDM algorithm (an explicit scheme is applied). The Stefan model and micro/macro one is considered (N = 10^{12} nuclei/m^3, $\mu = 3 \cdot 10^{-6}$ m/sK^2). Initial temperature of molten metal T_0 = 680°C, solidification point T^* = 660°C, initial temperature of mould T_{m0} = 20°C. The remaining input data are taken from [3].

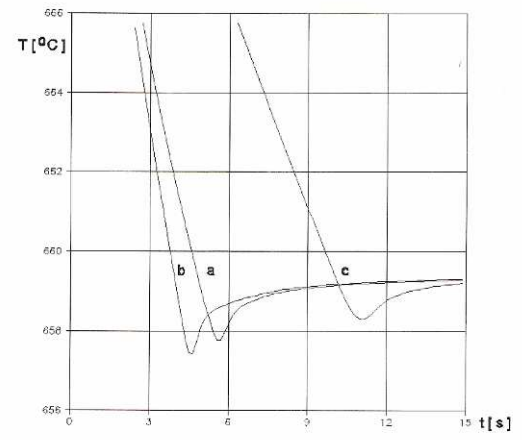

Fig. 5. Cooling curves at points a, b, c

In Figure 5 the cooling curves (micro/macro model) at the points a, b, c - as in Figure 4 are shown. The typical feature of the solution obtained on the basis of Kolmogoroff model is the visible undercooling below the solidification point. This phenomenon is confirmed by the numerous experiments.

The differences between the Stefan problem solution (for the same input data) and the micro/macro model are shown in Figures 6 and 7. The solid lines illustrate the changes of f_S corresponding to the micro/macro model while the symbols correspond to macro approach. The comparison concerns the function f_S because the temperature profiles are very close.

The solution of macro model has been found by coupling of FDM algorithm with TRM procedure. For aluminium the initial value of θ equals 325 K and the solidification process stops when local value of θ achieves 0. The TRM allows a certain free choice on a stage of f_S definition. It is possible to introduce the value being the ratio of temporary and local value of θ to its initial value

$$\mu = \frac{\theta - \sum_{k=0}^{f+1} \Delta \theta_0^k}{\theta} \tag{13}$$

and then function f_S fulfilling the condition $f_S \in [0,1]$ can be defined as follows

$$f_S = 1 - \mu^p \ , \quad p > 0 \tag{14}$$

In Figures 6 and 7 the changes of f_S at the points b, c for p = 1 and p = 3/4 are shown.

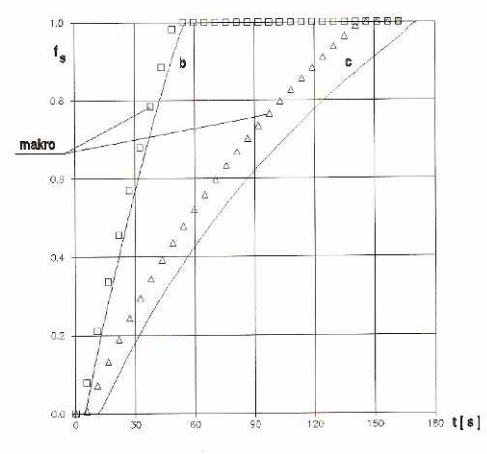

Fig. 6. Comparison of solidification kinetics (b, c), p = 1

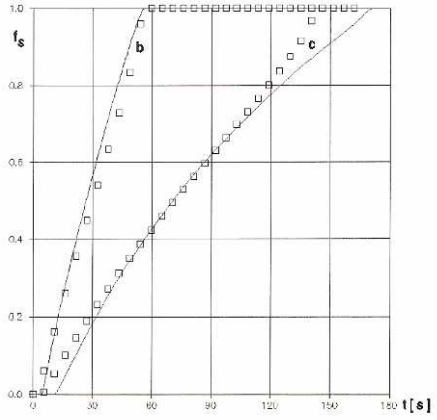

Fig. 7. Changed definition of f_S

One can see that assumption $p = 3/4$ assures a good conformability of both solutions, but the proper choice of p on a stage of input data definition is rather impossible. In spite of this the differences between two solutions presented even in the case $p = 1$ are not big. From the physical point of view the micro/macro approach is more exact and closer to the real course of solidification, but in practice the solution basing on the Stefan model is also acceptable.

References

[1] Longa W., Krzepnięcie odlewów, Śląsk, Katowice 1985.

[2] Crank J., Free and moving boundary problems, Claredon Press, Oxford 1984.

[3] Mochnacki B., Suchy S.J., Numerical methods in computations of foundry processes, PFTA, Cracow 1995.

[4] Szopa R., Modelling od Solidification and Crystallization using the Combined Variant of the BEM, Publ. of the Sil. Univ. of Techn., Metallurgy, 54, Gliwice 1999.

[5] Kapturkiewicz W., Modelling of Cast Iron Crystallization, AKAPIT, Cracow 2003.

[6] Szopa R., Macro and macro/micro models of solidification. Numerical aspects of process simulation, Materials Science Forum 2007, 539-543, 2564-2569.

[7] Mochnacki B., Szopa R., Model of pure metal solidification using the power-type function, Journal of Achievements of Materials and Manufacturing Engineering 2007, 22, 1, 65-68.

[8] Majchrzak E., Numerical simulation of continuous casting solidification by BEM, Engineering Analysis with Boundary Elements 1993, 11, 95-99.

[9] Lara S., Doctoral Theses, Częstochowa 2003.